

# NUMERICAL SIMULATION FOR IMPROVING A ROTARY MOTOR EFFICIENCY BY FLOW OPTIMIZATION INSIDE THE MOTOR'S CHAMBERS

**Savvas Savvakis, Zissis Samaras**

Aristotle University of Thessaloniki/Laboratory of Applied Thermodynamics, Greece

## KEYWORDS -

*ICE, rotary engine, thermodynamic analysis, quad meshing, hexahedral volumes*

## ABSTRACT -

A clear understanding of the flow inside the chambers of a rotary engine would help the optimization of the injection, vaporization and combustion quality in order to improve the efficiency of the whole operating cycle of the motor. The objective of the present project was to optimize the design of the chambers with the use of ANSA and CFD tools. The 3D-modelling and finite element analysis has been created by the preprocessor ANSA, while the thermodynamic analysis of the resulting model has been carried out by the CFD-solver Fluent.

The focus of the present contribution is put on the ability of ANSA to make hexahedral volumes of simple and complex designs. Although ANSA has been focused on creating triangle Finite Element Analysis of every possible geometry, it supports functions able to generate structured and unstructured fully hexahedral Finite Element Models (FEMs). The current presentation will show how quad surface mesh and hexahedral Grid may be applied in geometries, which seem complicated enough to be analyzed in a no tetrahedral volume mesh.

Finally, the presentation ends with an illustration of the motor's operating cycle as well as the overview of the thermodynamic analysis results.

## TECHNICAL PAPER -

### 1. INTRODUCTION

The increasing demands on engine power and performance to meet the ever increasing demands of the customers have necessitated the automotive manufacturers to invest considerable resources attempting to develop new combustion technologies and optimize the existing reciprocating internal combustion engines.

However, this type of engine has a significant disadvantage inherent in its operating principle. The disadvantage refers to the conversion of reciprocating to rotational motion. A mathematical and trigonometrical analysis, whose results are demonstrated in Figure 1, show that almost 80% of the mean torque that the pressure developed on the piston could theoretically give is lost during this conversion because of the position and angle of the connecting rod. This problem however cannot be avoided because of the reciprocating engine operation principle and this is a reason why the mean specific fuel consumption of this type of engine can not fall below 100 g/kWh.

In order to eliminate these losses, the current study proposes a rotary engine which inherently transports 100% of the theoretically developed torque to the engine shaft. However, this is a characteristic of all concentric rotary engines. The special feature of this one is the existence of a pressure chamber and the position of the pistons relative to the engine shaft.

---

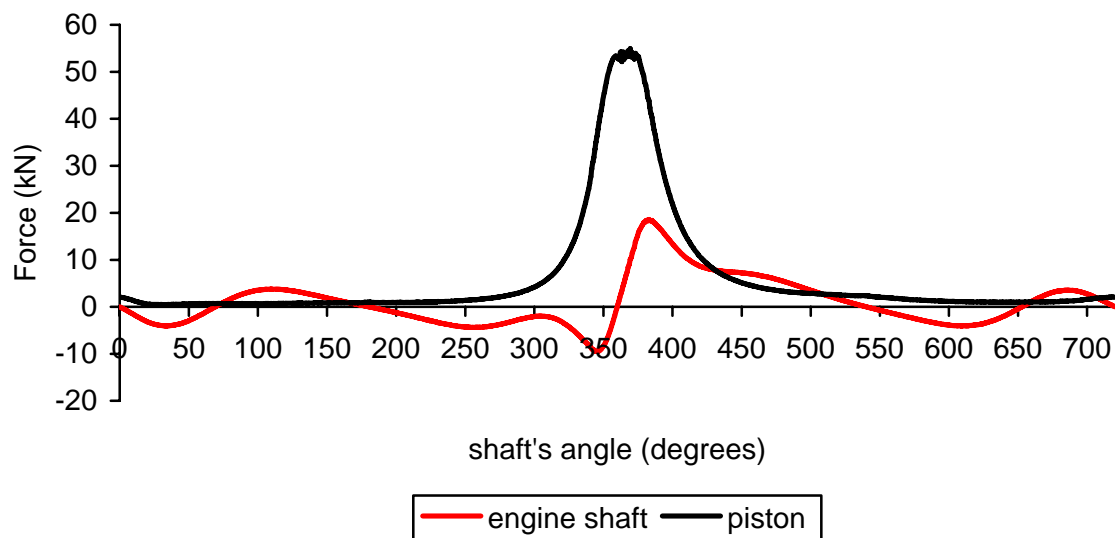


Figure 1. The force distribution on the piston and on the engine shaft of a Diesel Engine

## 2. THE PHYSICAL MODEL

This internal combustion rotary engine is a new concept of engine patented internationally (PCT Number GR2006/000027). This engine comprises one compression chamber designed to provide the intake and compression process, one combustion chamber that provides the combustion and expansion process, as well as one pressure chamber placed between the compression and combustion chambers and communicating with both of them. The pressure chamber stores air under high pressure charged by the compression chamber. The role of this chamber is to ensure the high pressure transport of the compressed air from the compression chamber to the combustion chamber. Additionally, its presence makes the initial combustion conditions independent from the intake and compression conditions, expands the injection and fuel-air mixing time as well as ensures a good mixing of the fuel with the combustion air.

Furthermore, the engine comprises two pistons, an expansion and a compression piston, moving in a circular orbit being. The combustion chamber hosts the expansion piston, while the compression chamber hosts the compression piston. The compression piston is directly attached on the engine shaft in order to minimize the distance of the compression piston from the engine shaft and subsequently the torque required for the motion of the piston and the compression of the intake air.

The engine also comprises a motion arm attachable to the engine shaft and a rotating wall having a ring configuration attached to the free edge of the motion arm, where the expansion piston is attached as well. The motion arm is set to motion by the expansion process and is moved from the expansion piston and subsequently transmits the motion to the engine shaft. The expansion piston is attached on the free edge of a motion arm since this configuration ensures that the expansion piston circular orbit will have a maximum rotation radius producing a maximum torque during the combustion and expansion of the air-fuel mixture.

The compression chamber is in contact with the cylindrical outer surface of the engine shaft, formed by the outer cylindrical surface of the engine shaft, a sliding port, the compression piston, and a stationary toroidal shell attached on the frame of the motor. The combustion chamber is formed by a sliding port, the expansion piston, two stationary toroidal shells attachable on the motor's frame and the aforementioned rotating wall.

The fluid communication between the pressure chamber and the combustion and compression chambers is controlled by valves, while a relief valve in the pressure chamber is used to prevent an increase of pressure inside the pressure chamber in case of high operation temperatures.

Figure 2 depicts the fluid-volumes of the chambers as well as all the moving parts of the engine. The different colours represent the five different chambers of the engine. More specifically, the dark blue corresponds to the intake chamber, the light blue to the compression chamber, orange is the pressure chamber and red the combustion chamber, while the yellow colour shows the expansion chamber as well as the exhaust pipe. The description of the engine that was done above referred to one chamber of each kind and one of each piston as well, but for a smoother operation avoiding the oscillations, a couple of each kind is used for the final model.

Finally, the five numbers in the Figure 17 have the following meanings:

- 1... compression piston
- 2... sliding ports
- 3... valves
- 4... rotating wall
- 5... combustion piston

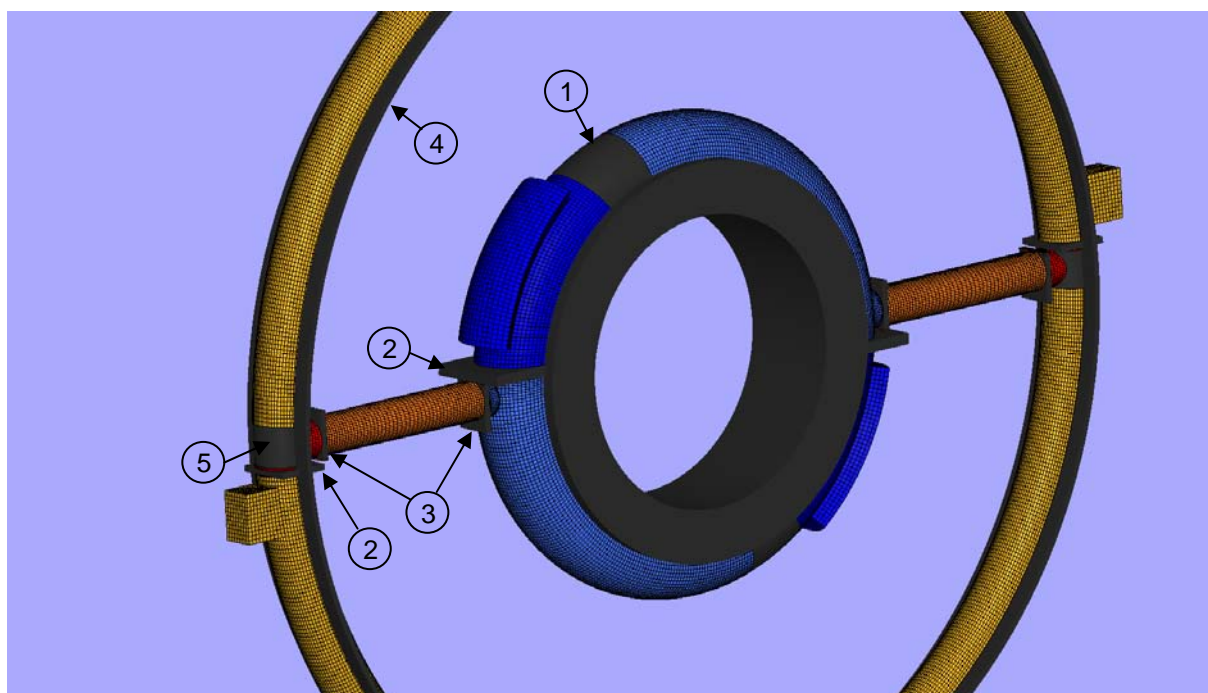


Figure 2. The fluid-volumes of the chambers and the moving parts of the engine

The operation of the engine comprises the following steps:

- opening of the sliding port of the compression chamber;
  - moving of the compression piston to create an area of low pressure, which forces atmospheric air to enter into the compression chamber through air filters;
  - covering of the entire volume of the compression chamber with atmospheric air;
  - closing of the sliding port of the compression chamber hence producing a volume of air between the sliding port and the compression piston ;
  - compression of the combustion air by moving further the compression piston ;
-

- opening of the compression chamber valve as soon as a predetermined pressure has been reached and allowing the transfer of combustion air from the compression chamber to the pressure chamber ;
- storing of the combustion air in the pressure chamber;
- opening of the combustion chamber valve, allowing the air to flow from the pressure chamber to the combustion chamber;
- moving of the combustion piston to create an area of low pressure that leads combustion air from the pressure chamber into the combustion chamber;
- closing of the combustion chamber valve ;
- fuel injection into the combustion chamber; and
- ignition of the air-fuel mixture either under constant pressure or under constant volume by at least one spark plug producing an exhaust gas which expands and pushes the expansion piston in a motion that moves the engine shaft which moves the compression piston.
- closing of the compression chamber valve as soon as the pressure in the compression chamber reaches a pre-defined value.

### 3. THE FINITE ELEMENT MODEL

#### 3.1 Comparison of a hexahedral mesh with a tetrahedral mesh

The 3D FE Model of this engine is focused on the hexahedral mesh because of the benefits that this mesh presents in comparison to other meshes. Higher accuracy of the solution and better approximation of the experimental results seems to be possible when the geometry consists of structured hexahedral mesh and the mesh is aligned with the flow direction.

On the other hand, the solution time, convergence and accuracy of the results of a simulation depend highly on the mesh quality. Highly skewed cells, which are frequently met in other than hexahedral meshes, harm convergence, often leading to solution divergence due to large source terms.

Moreover, highly stretched cells, which are rare in a hexahedral mesh, make the equations stiff delaying convergence considerably and, quite frequently, the solution diverges because of just a few problematic cells. For instance, in a case study with only seven problematic cells, the steady-state solution diverged after 73 iterations (1).

This kind of problematic cells is mostly generated by tetrahedral finite element analysis, imposing to pre-processors such as ANSA the use of a variety of functions and algorithms for checking the mesh quality and improving it, in order to avoid the divergence problems and the delay of the solution process.

Other parameters which impact mesh quality are cell size change (known as growth rate, too) and alignment with the flow, where the accuracy gap between quad/hex and tri/tet becomes much narrower, but remains significant enough. More specifically, the quad/hex mesh gives results very close to the experimental data only when the cells are aligned with the flow direction and the growth rate is less than 20%. The reason is that the truncation error for quad/hex cells is inherently lower than that of tri/tet cells, when they are aligned with the flow direction and the gradients of the transported variables.



The same conclusion is reached in another case study with 970K-cell hex mesh, 1.6M-cell tet mesh and 1.1M-cell hybrid (prism+tet) mesh, where the drag on a sphere was studied.

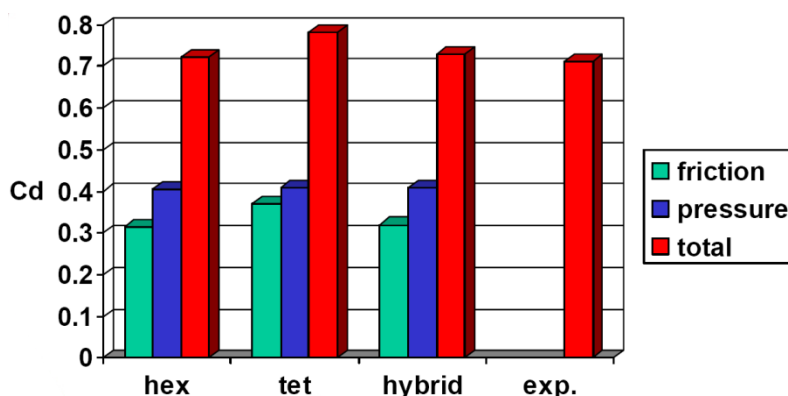


Figure 5. Comparison of the hexahedral, tetrahedral and hybrid (prism+tet) mesh with respect to the accuracy of the solution (1)

Solvers such as Fluent, in order to avoid structured and generally quad/hex meshes, but still maintain the benefits of a structured mesh, have appended to their code complicated and sophisticated algorithms such as Second-Order convective fluxes reconstruction, MUSCL scheme, bounded central differencing, node-based gradient scheme and others (2). In agreement with this guideline, ANSA has developed functions which automatically check and correct problematic elements, improve grid quality and enhance the convergence trend of the solution. Some of these ANSA functions are the Reconstruction, Distortion and Smoothing Button (3).

Here, somebody may ask the question what would happen if the developers focused on the creation of automated quad/hex meshes rather than trying to solve the problems generated from the tri/tet meshes. Up to now, significant improvements have been made in automatically detecting and correcting problematic areas, as well as reconstructing locally the geometry to avoid high skewness and extreme aspect ratios. All these functions and algorithms have been based on the experience of expert users. Would we have the same result in the case the focus was not "healing" a bad mesh quality but creating from scratch a "healthy" one?

Having this approach in mind and the great benefits of hexahedral mesh, there was a persistent endeavor to create the mesh of the new concept rotary engine fully of hexahedral cells. This effort has born its fruits and, with the aid of ANSA, a group of methodologies and techniques was developed, based on experience, which led to the creation of a pure hexahedral mesh of the whole engine, including both the working fluid and the solid parts.

### 3.2 The mesh of the rotary engine

The surface and volume mesh were generated using ANSA™ the use of which for surface meshing reduced significantly the CFD cycle time.

Figures 6 to 13 demonstrate the engine's solid parts while figures 14 to 17 show the working fluid that takes part in the operating cycle.

The non-conformal interfaces that have been used in the case of the fluids are decided in order to avoid the reconstruction of the mesh, every time the pistons pass by the pressure chamber ensuring the use only of the layering dynamic mesh motion method and avoiding thus the other available time-consuming methods.

The mesh of the pressure chamber, shown in figures 15 &16, is not the final mesh that has been used, but essentially represents the ability of ANSA to make automatically such changes in the quad cells direction without the need to insert tetrahedral or prism cells in between.

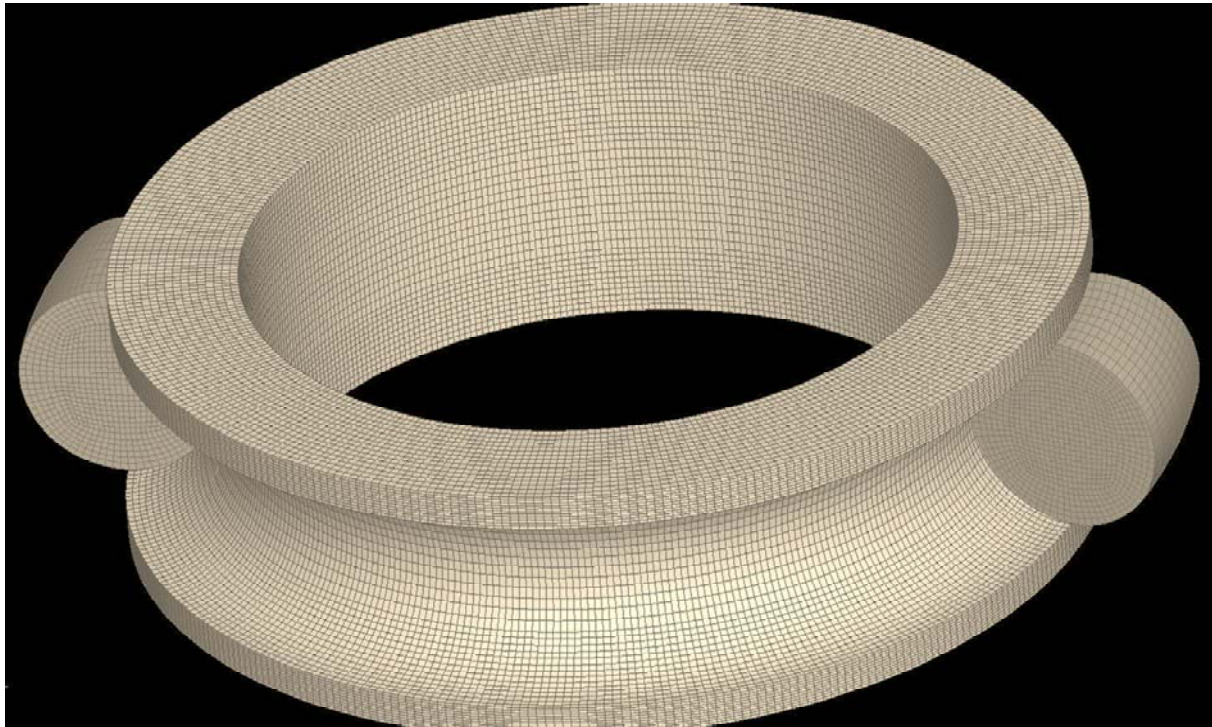


Figure 6. The FEM Analysis of the solid part called compression chamber

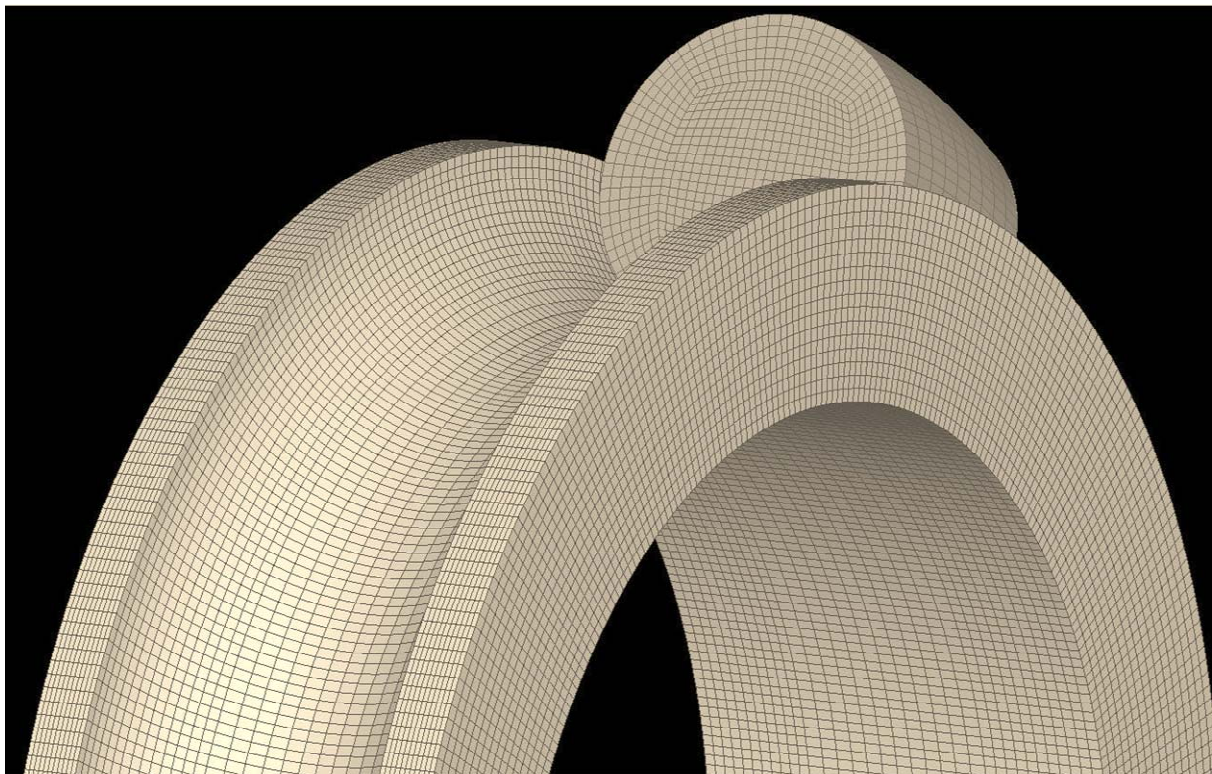


Figure 7. A more close view of the compression piston, which shows better its meshing

---

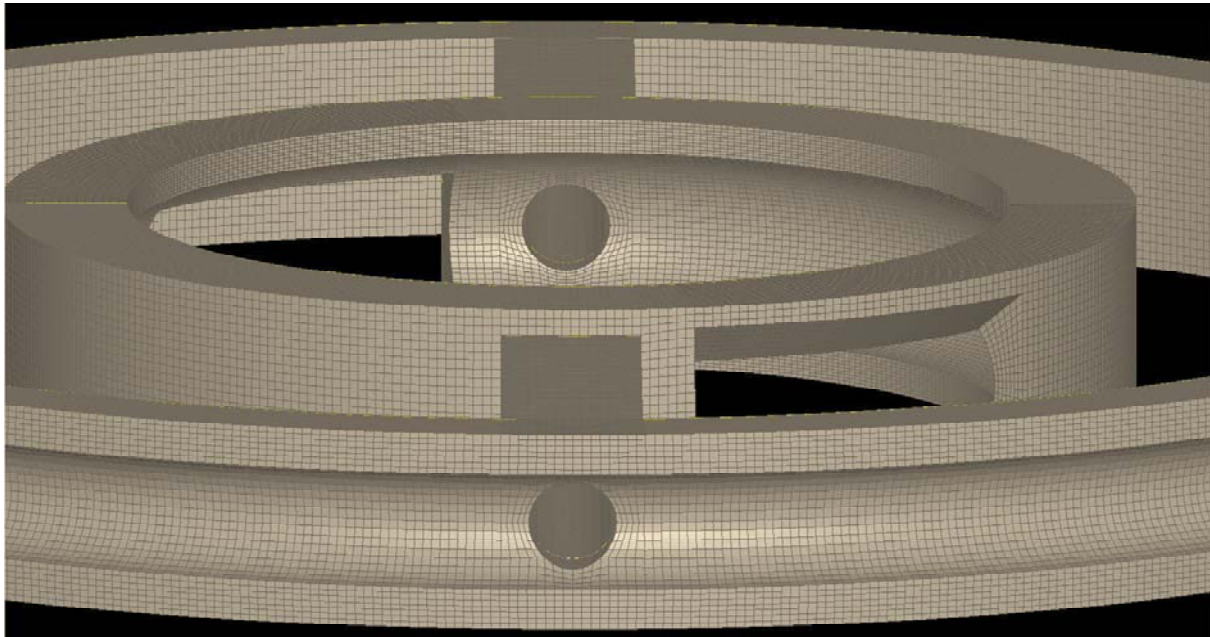


Figure 8. The FEM Analysis of the solid part called pressure chamber

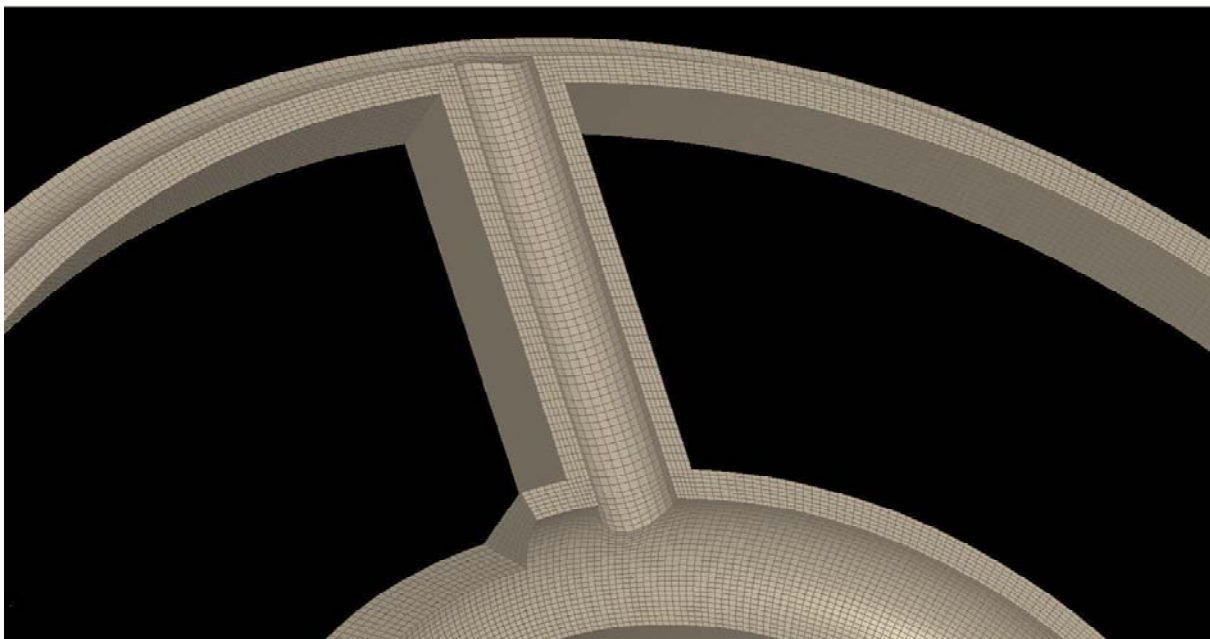


Figure 9. A section of the pressure chamber

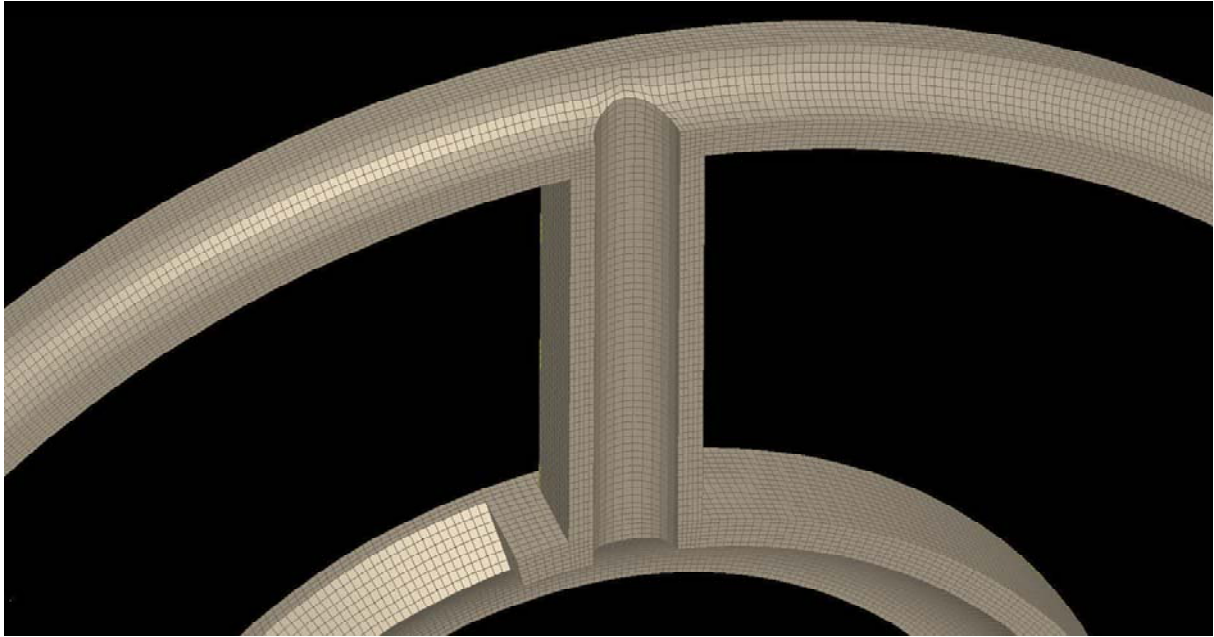


Figure 10. The same section as shown in figure 9 from another point of view

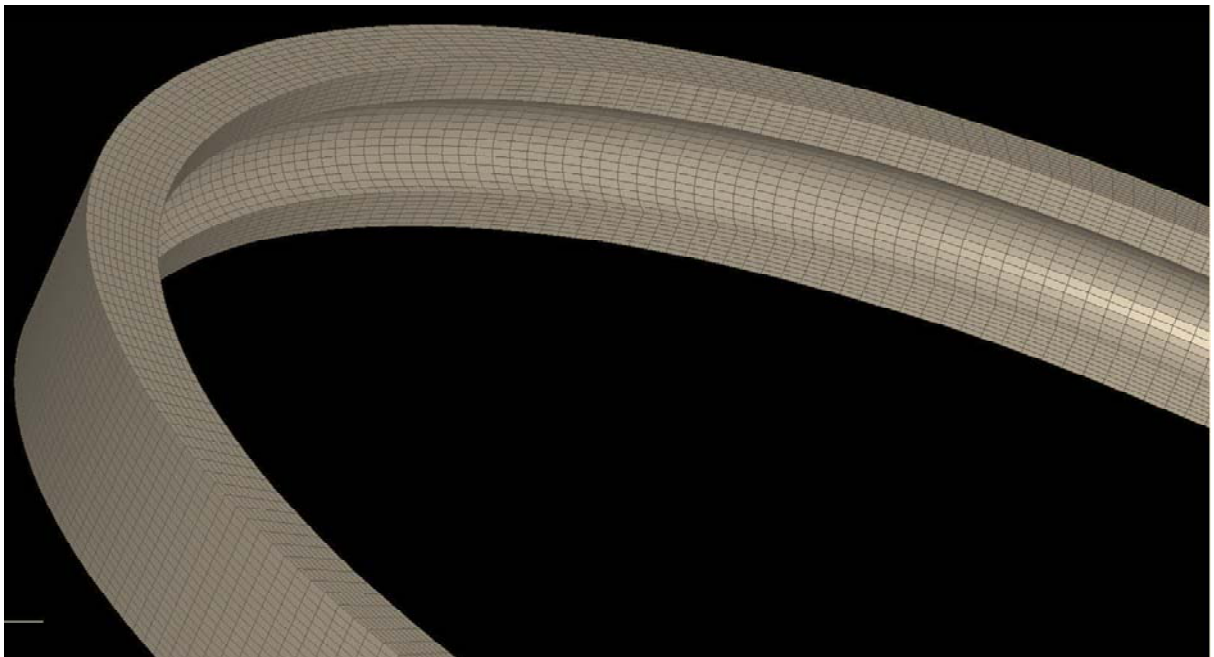


Figure 11. The FEM Analysis of the upper end part of the rotary engine whose role is to ensure that the combustion and expansion chamber will be airtight

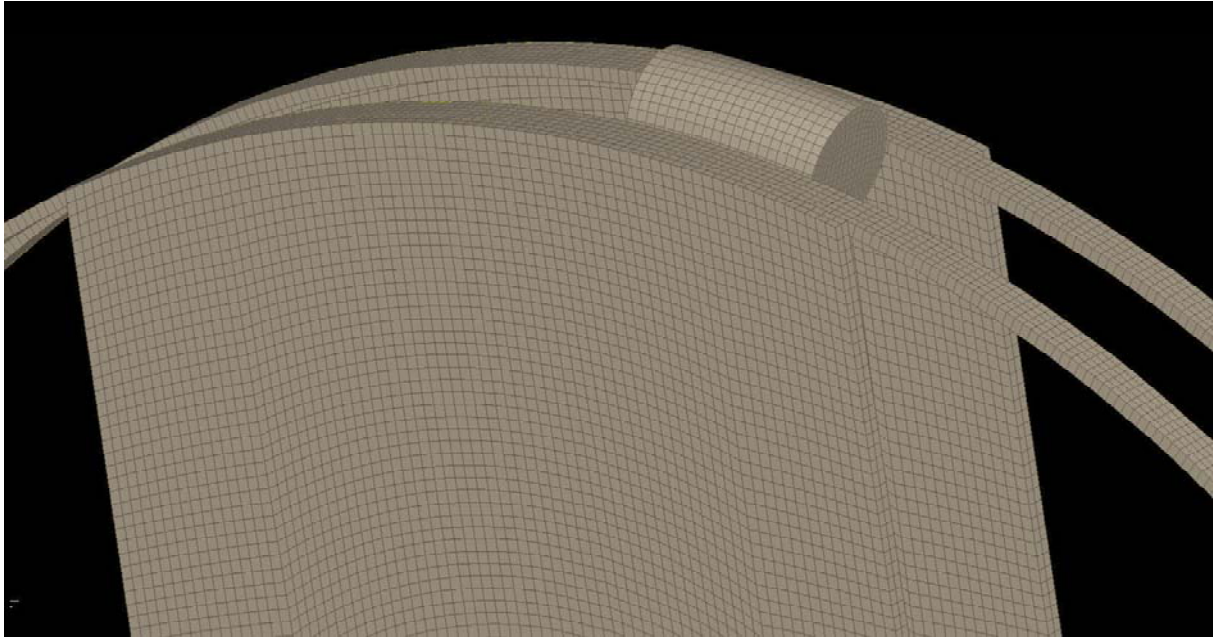


Figure 12. The FEM Analysis of the combustion piston.

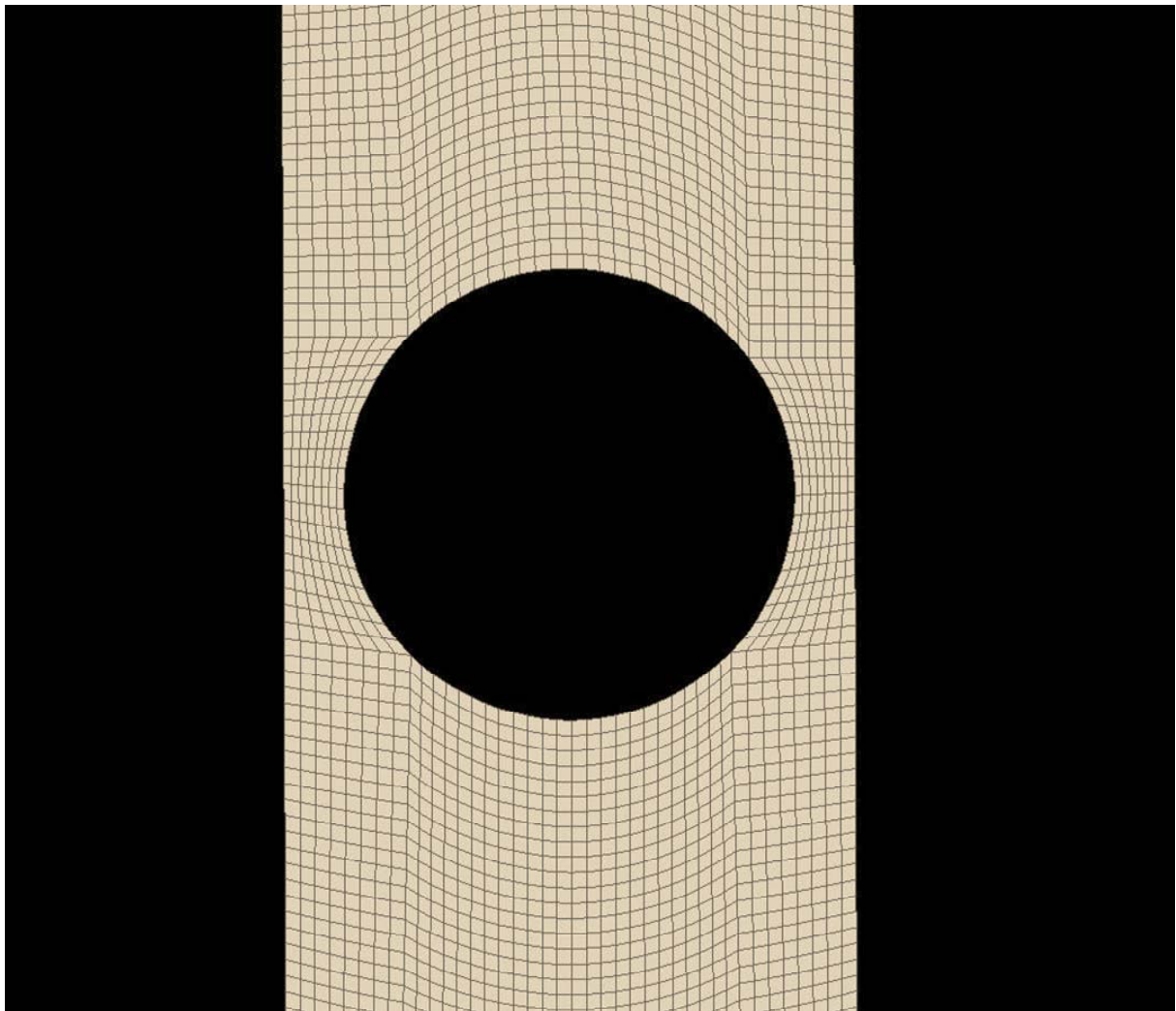


Figure 13. The position where the motion arms fit around the engine shaft.

---

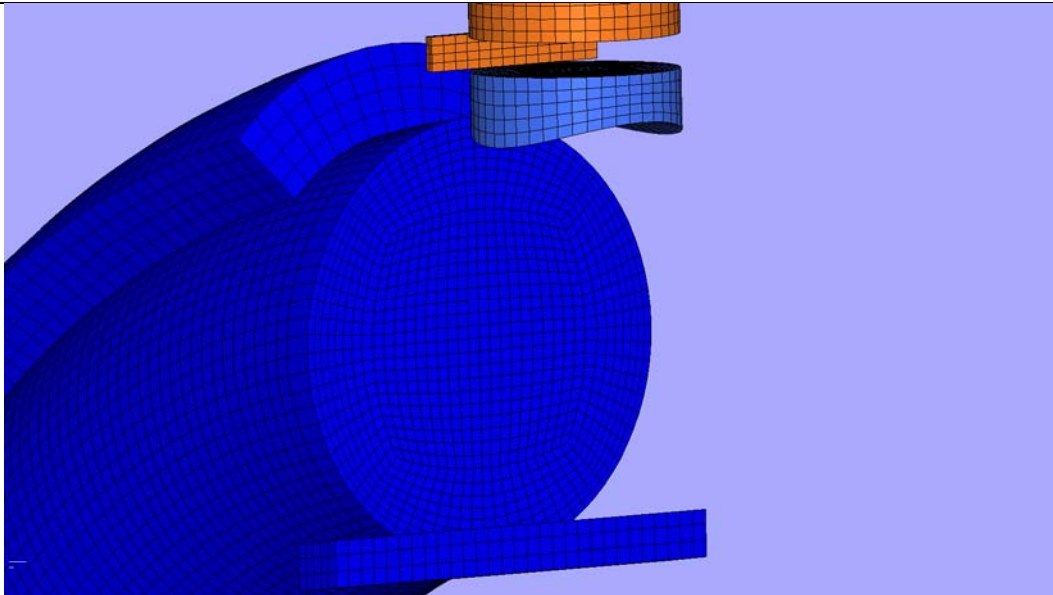


Figure 14. FEM analysis of the working fluid (intake chamber)

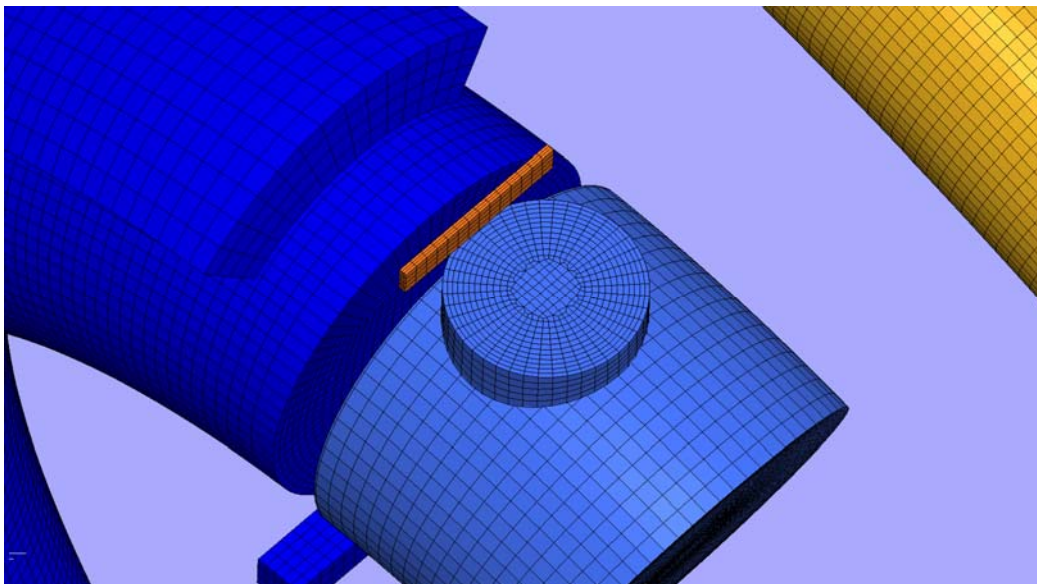


Figure 15. FEM analysis of the working fluid (compression chamber)

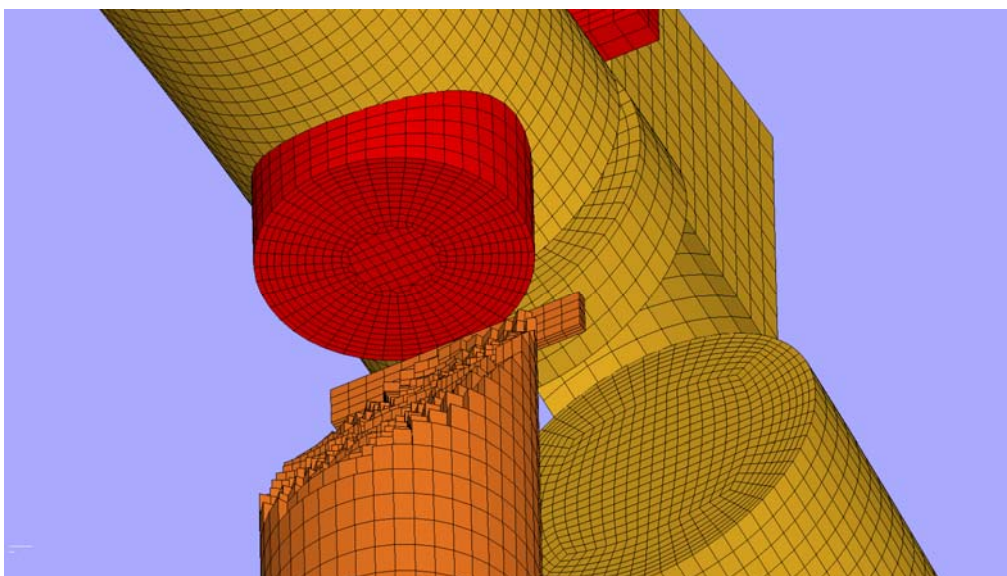


Figure 16. FEM analysis of the working fluid (combustion chamber)

---

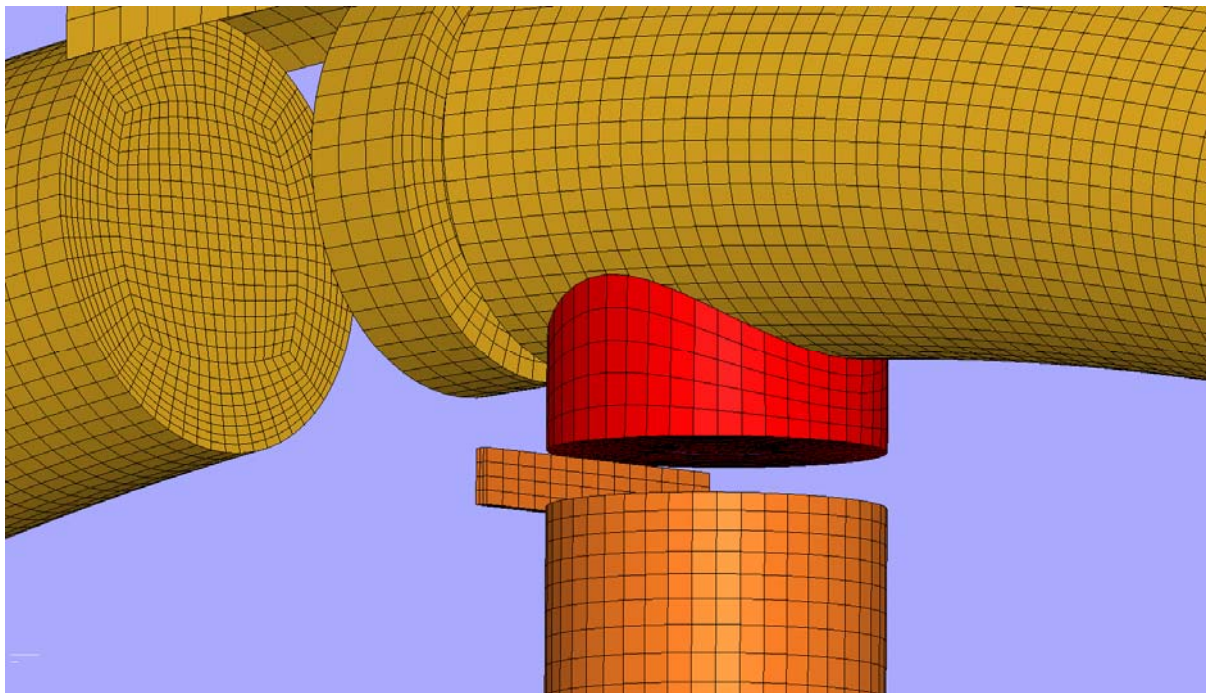


Figure 17. FEM analysis of the working fluid (expansion chamber)

#### 4. NUMERICAL MODEL

After both the 3D CAD model and the grid were built in ANSA, the numerical model was developed using the commercial solver FLUENT putting the appropriate factors for scaling the mesh/geometry, setting up the appropriate turbulence model, fluid properties, solver controls, convergence monitors, etc.

A segregated pressure-based solver was used for transient time with absolute velocity formulation. All simulations were performed using the RNG variant of the k- $\epsilon$  turbulence model with standard wall functions for near wall treatment and a second order upwind differencing scheme for all variables.

Other assumptions:

- The working medium was assumed to be dry air behaving as ideal gas.
- All walls were assumed to be thermally insulated and thus adiabatic.
- A partially premixed combustion model was applied
- Fixed spark ignition model was used whose shape assumed to be a sphere
- The injection type was cone with particle type of droplets, while the injected medium was n-octane liquid with rosin-rammler diameter distribution
- The dynamic mesh method was layering for moving walls
- PISO Algorithm was used for Pressure – Velocity Coupling and, finally,
- PRESTO! Spatial Discretization for Pressure was used

#### 5. SIMULATION RESULTS

Modelling the base case, whose operating cycle has been described above, resulted in the torque distribution that is presented with the black line in Figure 18. For this operating cycle, the amount of the injected fuel was 30 mg per revolution.

---

The current operating cycle has been repeated for two continuous revolutions and it was observed that the torque distribution of the second rotation was the same with the first one. This indicates that the pressure chamber makes the initial conditions of every rotation independent of the previous rotations and thus the turbulence of the intake and pressure process do not influence the process of fuel injection and combustion.

After that, three study cases were built and run for flow and efficiency optimization.

In the first case study, the engine has been solved without fuel injection and spark ignition, studying only the pure fresh air compression and expansion in order to investigate the influence of valve timing to the air turbulence inside the combustion chamber (series of scenarios 1.x).

For the best valve timing and air turbulence inside the combustion chamber, the second case study was run, where the engine was simulated once again taking into consideration fuel injection, in order to investigate the best injector position and orientation (series of scenarios 2.x).

After the injector position and orientation were defined, the engine was finally simulated taking into consideration the ignition process for different spark positions in order to investigate the best spark position for an easy engine construction and a rapid combustion process (series of scenarios 3.x).

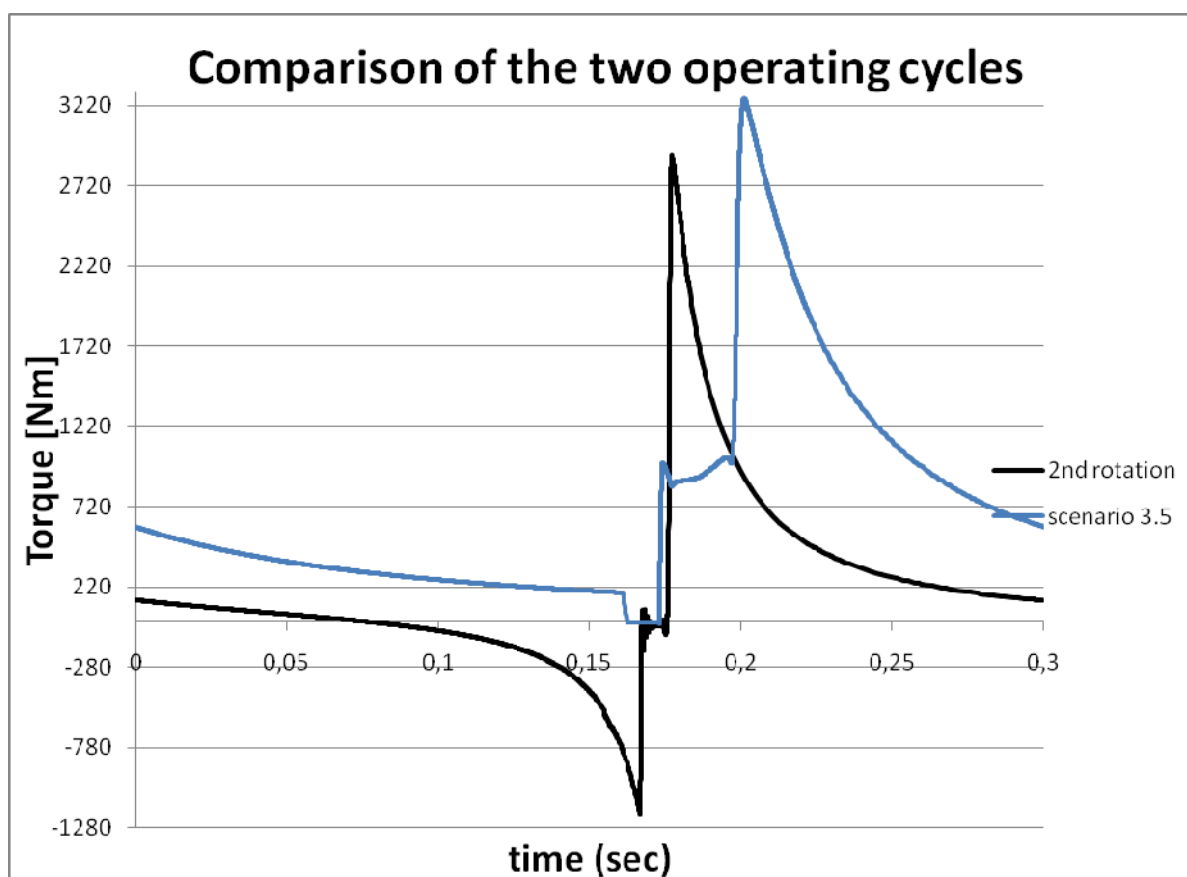


Figure 18. Comparison of the initial and final operating cycle based on the torque distribution

The last Figure shows the up to now best solution (scenario 3.5) whose settings are the following:

velocity: 100 rpm

mean torque: 520 Nm

engine capacity: 920 cm<sup>3</sup>

Power: 5.5 kW

fuel injection: 58,6 mg/revolution (almost the double of the base case)

injection time: 6.82 msec (the same injection time with the base case)

The essential difference of the two operating cycles is the valve timing and the injection process.

In the last scenario, the valves are not synchronized. They are controlled independently and, more specifically, the valve which puts the pressure chamber in communication with the combustion chamber, called combustion valve, opens before the other valve, called compression valve, and closes at the same time and in the same time period with the latter.

Finally, the injection is taking place inside the pressure chamber. It starts when the combustion valve starts to open and finishes just before the two valves close. This gives an extra time to the injected fuel to be evaporated and get mixed with the compressed air.

In scenario 3.5, whose torque distribution is depicted in Figure 18, just before the spark ignition, the macroscopic relative air/fuel ratio inside the combustion chamber is 1.4-1.6.

## 6. CONCLUSIONS

The Finite Element Analysis with the aid of ANSA and Computational Fluid Dynamics Analysis with the aid of Fluent enabled the improvement of the new concept rotary engine's operating cycle.

Starting from a validation solution of the baseline design, a first optimization of the engine was carried out. The analysis of the final optimized configuration shows a 25% improvement of the mean torque. On the other hand, this study showed that ANSA has all the functions required to fully design a 3D model and carry out its hexahedral Finite Element Analysis.

The next step will be the design optimization of the model with the support of ANSA's morphing tool and after that heat transfer effects and pollutant emissions will be incorporated into the current CFD model.

## REFERENCES

- (1) 2004 CFD SUMMIT TRAINING Dr. Sung-Eun Kim, Dr. Tiberiu Barbat and Dr. Peter Spicka
  - (2) Fluent version 12 User's Guide, ANSYS, February 2008
  - (3) ANSA version 12.1.5 User's Guide, BETA CAE Systems S.A., July, 2008
-